

Supporting Information

Accurate Assembly of Ferrocene-Functionalized $\{\text{Ti}_{22}\text{Fc}_4\}$ Cluster with Photocatalytic Amines Oxidation Activity

Er-Meng Han,^{a‡} Wei-Dong Yu,^{b‡} Jiao-Lei Li,^c Xiao-Yi Yi,^a Jun Yan^a Chao Liu^{a*}

^a Hunan Provincial Key Laboratory of Chemical Power Sources, College of Chemistry and Chemical Engineering, Central South University, Changsha 410083, Hunan, P. R. China

^b Hunan Institute of Nuclear Agricultural Science and Space Breeding, Hunan Academy of Agricultural Science, Changsha 410000, P. R. China.

^c Jilin Provincial Science and Technology Innovation Center of Optical Materials and Chemistry, School of Chemical and Environmental Engineering, Changchun University of Science and Technology, Changchun, Jilin 130022, China

*(Chao Liu) E-mail: chaoliu@csu.edu.cn

1. Experimental section

Materials and Characterization. All reagents were purchased commercially and were not further purified before use. Powder X-ray diffraction (PXRD) analysis was performed on a Rigaku Mini Flex II diffractometer at a 2θ range of $5\text{--}50^\circ$ (5°min^{-1}) with $\text{CuK}\alpha$ radiation ($\lambda = 1.54056 \text{ \AA}$). The solid-state UV/Vis spectra of the cluster samples were obtained on UV-4000 spectrophotometer. Fourier transform infrared spectroscopy (FTIR) data ($4000\text{--}400 \text{ cm}^{-1}$) was collected on a PerkinElmer Spectrum 100 FT-IR Spectrometer. Thermogravimetric analyses (TGA) were performed on a Mettler Toledo TGA/SDTA 851e analyzer in N_2 at a temperature range of $50\text{--}800^\circ\text{C}$ ($10^\circ\text{C min}^{-1}$). Crystallographic data for this article were obtained on a Bruker Apex II CCD diffractometer with graphite-mono-chromated Mo/Cu K α radiation. The structures were solved by direct methods and refined on F^2 by full matrix least-squares using new SHELXL program. All of the non-hydrogen atoms are located from Fourier maps and are refined anisotropically.

Synthesis of cluster $[\text{Ti}_5(\text{u}_3\text{-O})_3(\text{O}^i\text{Pr})_9(\text{Fdc})(\text{Dmg})(\text{Pdc})]$ (Ti_5Fc). DmgH_2 (17 mg, 0.147 mmol), FdcH_2 (55.2 mg, 0.24 mmol), 2,3-pyrazine dicarboxylic acid (18.6 mg, 0.1 mmol) and 3 mL isopropanol were added into a 25 mL Teflon lined stainless steel autoclave, and then combined with $\text{Ti}(\text{O}^i\text{Pr})_4$ (300 μL , 0.975 mmol). The solution was sonicated for 5 min, then transferred to an oven at 100°C for 3 days. After cooling to room temperature, yellow block crystals of $\{\text{Ti}_5\text{Fc}\}$ were obtained and washed with acetonitrile, then dried at room temperature. Yield: about 120 mg.

Synthesis of clusters $[\text{Ti}_{11}(\text{u}_3\text{-O})_9](\text{O}^i\text{Pr})_{12}(\text{Fdc})_2(\text{Dmg})_5$ ($\text{Ti}_{11}\text{Fc}_2$) and $[\text{Ti}_{22}(\text{u}_3\text{-O})_{18}](\text{O}^i\text{Pr})_{30}(\text{Fdc})_4(\text{Dmg})_7$ ($\text{Ti}_{22}\text{Fc}_4$). DmgH_2 (17 mg, 0.147 mmol), FdcH_2 (55.2 mg, 0.24 mmol), and 5 mL isopropanol were added into a 25 mL Teflon lined stainless steel autoclave. Then $\text{Ti}(\text{O}^i\text{Pr})_4$ (300 μL , 0.975 mmol) was added and transferred to an oven at 100°C for 3 days. After cooling to room temperature, yellow needle-like crystals of $\{\text{Ti}_{22}\text{Fc}_4\}$ and yellow plate-like crystals of $\{\text{Ti}_{11}\text{Fc}_2\}$ were obtained in about 3:1 ratio. The two crystals are very different in color and shape, and can be separated manually. Total yield: about 80 mg.

Individual synthesis of the cluster $\{\text{Ti}_{22}\text{Fc}_4\}$. DmgH_2 (35 mg, 0.3 mmol), FdcH_2 (55.2 mg, 0.24 mmol), benzoic acid (29.3 mg, 0.24 mmol) or isonicotinic acid (29.5 mg, 0.24 mmol), and 5 mL isopropanol were added into a 25 mL Teflon lined stainless steel autoclave. Then $\text{Ti}(\text{O}^i\text{Pr})_4$ (300 μL , 0.975 mmol) was added and transferred to an oven at 100°C for 3 days. After cooling to room temperature, yellow needle-like crystals of $\{\text{Ti}_{22}\text{Fc}_4\}$ were obtained, and only a very small amount of plate-shaped crystals of $\{\text{Ti}_{11}\text{Fc}_2\}$ was found in the mother liquor. Total yield: about 75 mg.

Individual synthesis of cluster $\{\text{Ti}_{11}\text{Fc}_2\}$. DmgH₂ (35 mg, 0.3 mmol), FdcH₂ (55.2 mg, 0.24 mmol), and 6 mL isopropanol were added into a 25 mL Teflon lined stainless steel autoclave. Then Ti(OⁱPr)₄ (500 μL, 1.63 mmol) was added and transferred to an oven at 120 °C for 3 days. After cooling to room temperature, a small amount of yellow plate-like crystals of $\{\text{Ti}_{11}\text{Fc}_2\}$ was obtained (Yield: about 30 mg). However, almost no plate-like crystals of $\{\text{Ti}_{11}\text{Fc}_2\}$ were found in the mother liquor.

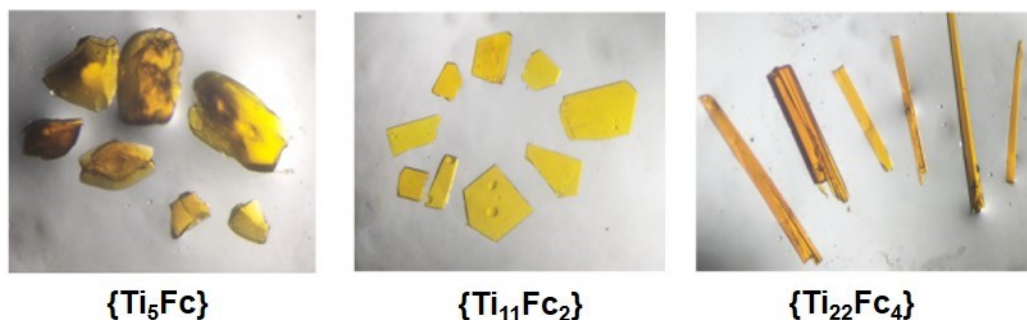


Figure S1. Crystal pictures of the clusters.

Photoelectrochemical measurements were performed on a CHI 660e electrochemical workstation in a standard three-electrode electrochemical cell with a working electrode, a platinum plate as the counter electrode, and a saturated calomel electrode as the reference electrode. These three electrodes were immersed in the 0.2M Na₂SO₄ aqueous solution (pH = 6.6). A 300 W high-pressure xenon lamp with UV cut-off filter was used as a full-wavelength light source, located 20 cm away from the working electrode. The on-off cycling irradiation intervals are 20 s. The working electrode was prepared on fluorinedoped tin oxide (FTO) glass. The colloidal dispersion was obtained by ultrasonic treatment of 5 mg ground crystal sample in 1 ml ethanol for 30 min, and then the dispersion was dropped onto FTO glass (0.75 cm² area). After evaporation under an ambient atmosphere for 2 h, the coating film was obtained and used as the working electrode.

Typical procedure for the oxidation of amines. The photocatalytic reactions were carried out under irradiation by a Xe lamp (300 W, PLS-SXE 300, Beijing Trusttech Co.) equipped with a cutoff filter to filter out light below 420 nm and a broad band filter to cutoff light above 750 nm, with magnetic stirring in a 10 mL Pyrex glass bottle. The bottle was sealed with a rubber stopper wrapped in aluminum foil. Benzylamine (1 mmol), catalyst (0.02 mmol), TBHP (300 mL) and solvent (2 mL) were added in a glass bottle. The reaction was stirred at 70°C under irradiation from the Xe lamp. After reaction, the mixtures were analyzed by GC and ¹H NMR. The catalysts were collected by filtration and washed with CH₃CN, and reused for the subsequent catalytic reactions.

2. Structure of Compounds

Table S1. X-ray measurements and structure solution of compounds.

| Compounds | $\{\text{Ti}_5\text{Fc}\}$ | $\{\text{Ti}_{11}\text{Fc}_2\}$ | $\{\text{Ti}_{22}\text{Fc}_4\}$ |
|---|---|---|--|
| CCDC | 2053563 | 2053564 | 2053565 |
| Formula | C ₅₃ H ₈₅ N ₃ O ₂₂ Ti ₅ Fe | C ₈₃ H ₁₃₇ N ₁₀ O ₃₉ Ti ₁₁ Fe ₂ | C ₁₆₆ H ₂₇₄ N ₁₂ O ₈₀ Ti ₂₂ Fe ₄ |
| F _w | 1411.58 | 2537.62 | 4994.27 |
| Crystal system | Triclinic | monoclinic | triclinic |
| Space group | P-1 | P2 ₁ /c | P-1 |
| a, Å | 13.5246(11) | 21.8611(6) | 22.0941(6) |
| b, Å | 14.1422(11) | 21.3692(5) | 22.6404(7) |
| c, Å | 20.7800(15) | 25.6759(9) | 25.2924(8) |
| α/° | 78.353(3) | 90 | 114.7150(10) |
| β/° | 76.753(2) | 110.058(3) | 95.4110(10) |
| γ/° | 63.302(2) | 90 | 91.8360(10) |
| V, Å ³ | 3433.9(5) | 11267.1(6) | 11405.8(6) |
| Z | 2 | 4 | 2 |
| ρ _{calcd} (gcm ⁻³) | 1.365 | 1.468 | 1.447 |

| | | | |
|--|---------------|---------------|----------------|
| μ (mm ⁻¹) | 0.829 | 8.938 | 1.048 |
| F(000) | 1472.0 | 5124.0 | 5134.0 |
| Data/restraints/parameter | 13385/78/879 | 20948/88/1351 | 39999/283/2698 |
| Goof | 1.022 | 1.031 | 1.073 |
| R ₁ /wR ₂ (I > 2 σ (I)) | 0.0474/0.1186 | 0.0675/0.1689 | 0.0858/0.2366 |
| R ₁ /wR ₂ (all data) | 0.0640/0.1335 | 0.1018/0.1951 | 0.1631/0.2683 |

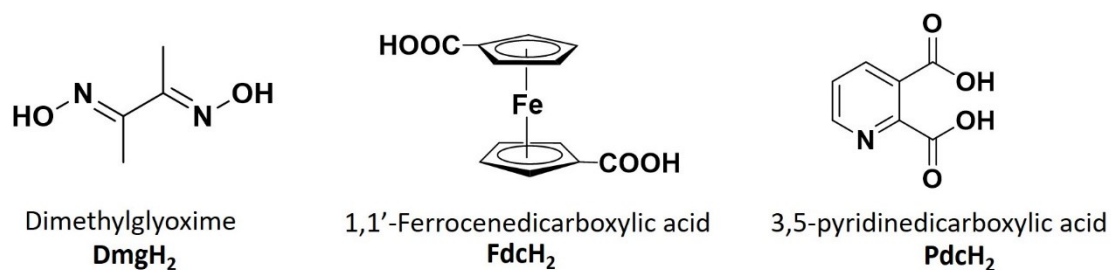


Figure S2. The molecular structures of all three ligands used in this work.

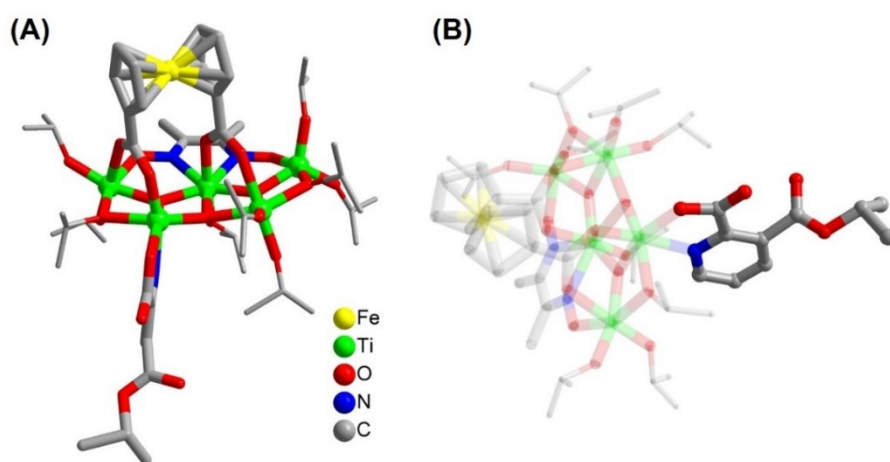


Figure S3. (A) Crystal structure of the cluster $\{\text{Ti}_5\text{Fe}\}$. (B) Pdch²⁻ ligand has three coordination groups, which are bonded to the Ti₅ layer through a pyridine N and a carboxylic O. Interestingly, another uncoordinated carboxylic group reacts with the isopropanol molecule in situ to form an ester bond.

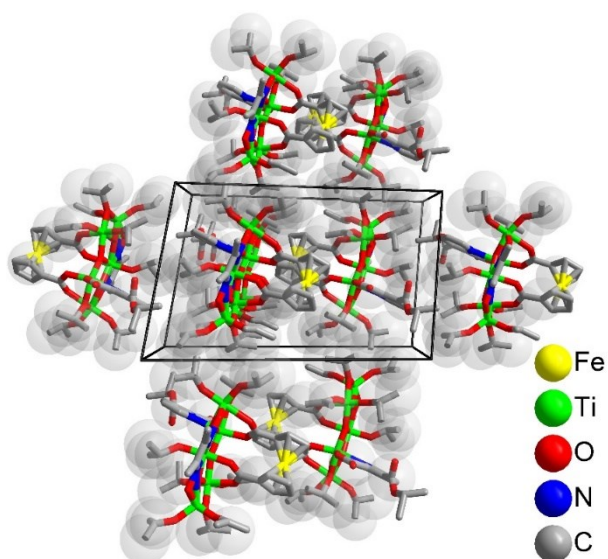


Figure S4. Three-dimensional packing structure of the cluster $\{\text{Ti}_5\text{Fc}\}$.

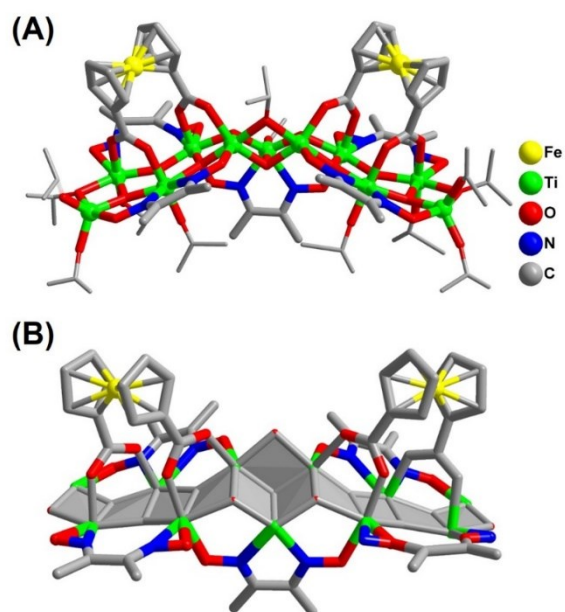


Figure S5. (A) Crystal structure of $\{\text{Ti}_{11}\text{Fc}_2\}$. (B) The simplified $\{\text{Dmg}_7\text{@Fdc}_2\text{@Ti}_{11}\}$ unit in $\{\text{Ti}_{11}\text{Fc}_2\}$.

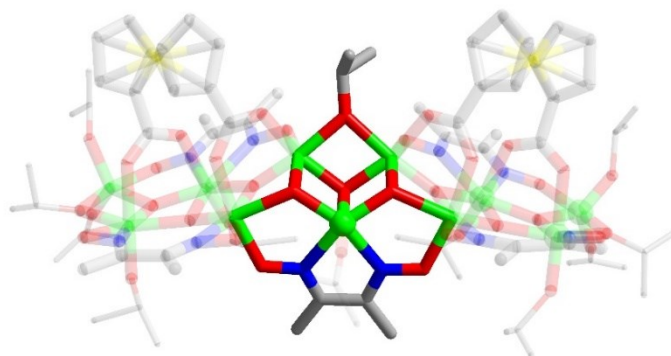


Figure S6. Two $\{\text{Ti}_5\text{Fc}\}$ subunits are bridged together by one $\{\text{Dmg@Ti}\}$ unit, three $\mu_3\text{-O}^{2-}$ atom and one O^{*i*}Pr group.

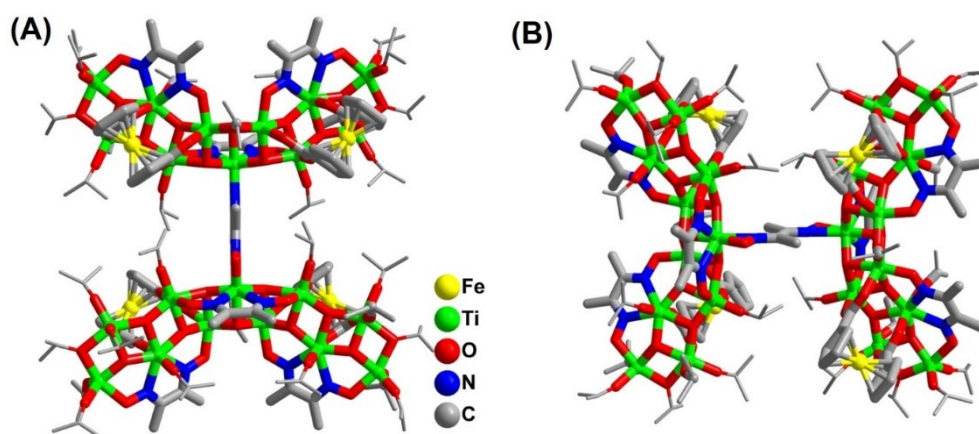


Figure S7. Two different perspectives of the crystal structure of $\{\text{Ti}_{22}\text{Fc}_4\}$

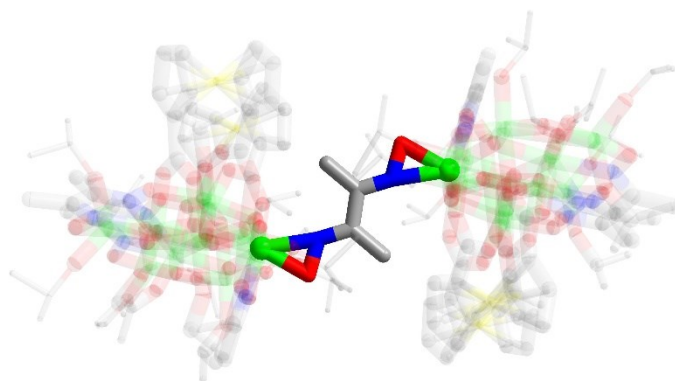


Figure S8. The big $\{\text{Ti}_{22}\text{Fc}_4\}$ structure can be viewed as two $\{\text{Dmg}_3@\text{Fdc}_2@\text{Ti}_{11}\}$ half-clusters linked through a trans- Dmg^{2-} ligand.

3. XPS spectra of $\{\text{Ti}_{22}\text{Fc}_4\}$

The XPS spectra of $\{\text{Ti}_{22}\text{Fc}_4\}$ shows that the Ti 2p spectra has two peaks with binding energies of 457.6 and 463.6 eV, representing the $2p^{2/3}$ and $2p^{1/2}$ states of Ti(IV) respectively, while the Fe 2p peaks with binding energies of 706.9 and 719.6 eV correspond to electrons in the $2p^{2/3}$ and $2p^{1/2}$ states of Fe(II), respectively.

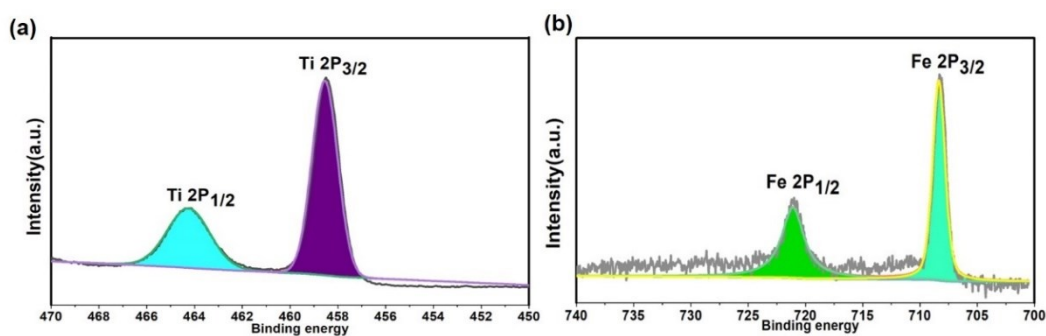


Figure S9. The XPS spectra of $\{\text{Ti}_{22}\text{Fc}_4\}$.

4. Powder X-ray diffraction

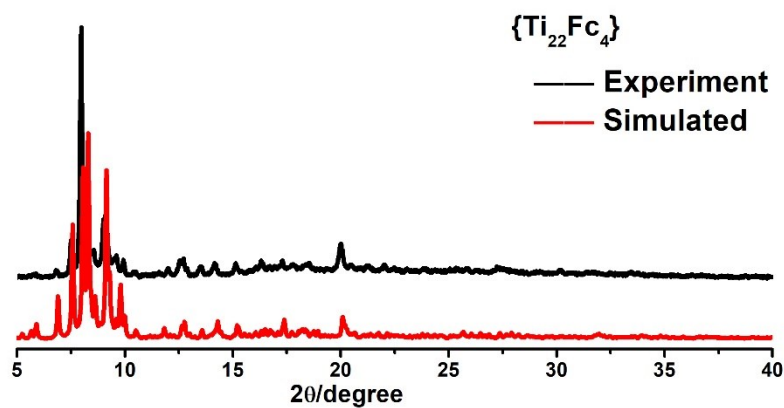


Figure S10. The XRD patterns of $\{\text{Ti}_{22}\text{Fc}_4\}$.

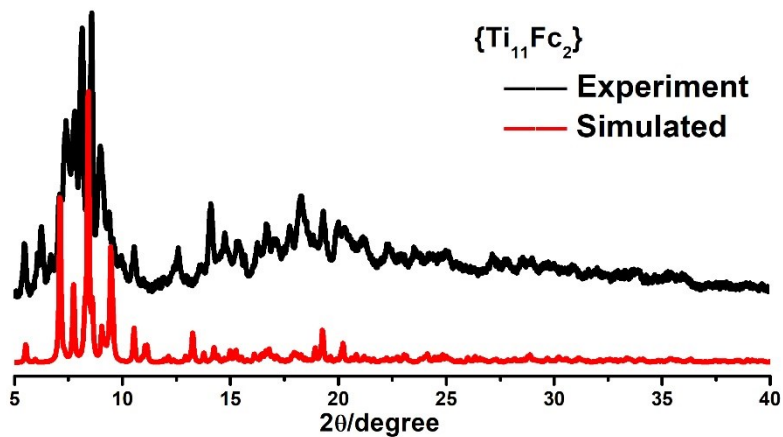


Figure S11. The XRD patterns of $\{\text{Ti}_{11}\text{Fc}_2\}$.

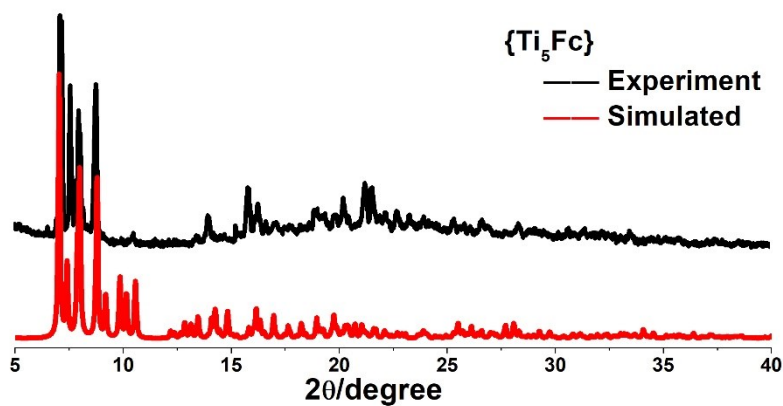


Figure S12. The XRD patterns of $\{\text{Ti}_5\text{Fc}\}$.

5. EDS patterns

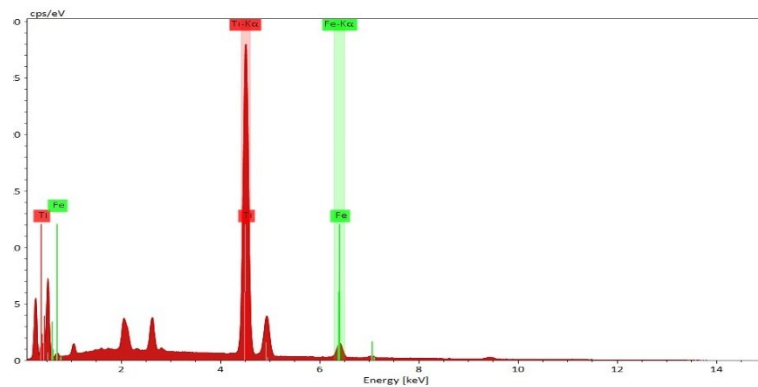


Figure S13. The EDS patterns of $\{\text{Ti}_5\text{Fc}\}$.

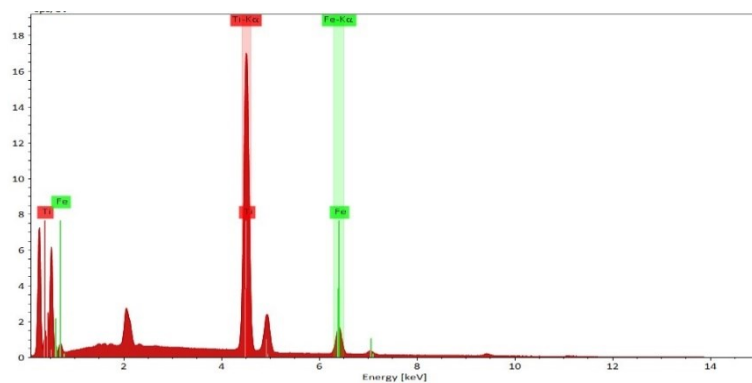


Figure S14. The EDS patterns of {Ti₁₁Fc₂}.

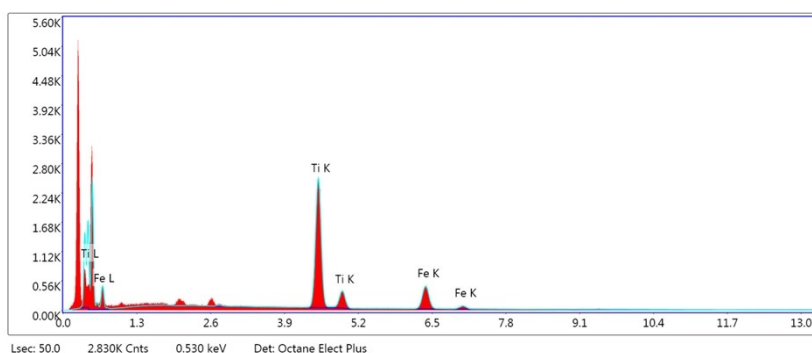


Figure S15. The EDS patterns of {Ti₂₂Fc₄}.

6. IR spectra

Figure S20-22 shows the FTIR spectra of three clusters. The broad band between 3200-3500 cm⁻¹ attributable to OH stretching. The strong vibration band at ca. 1620-1650 cm⁻¹ can be ascribed to C=O stretching of the Fdc²⁻ ligand. The characteristic bands of Ti-O-C and Ti-O-Ti appears in the ranges of 1000–1200 and 700–800 cm⁻¹, respectively. The characteristic peak of Fe-C vibration of the fFdc²⁻ ligand appears in the ranges of 500–600 cm⁻¹, respectively.

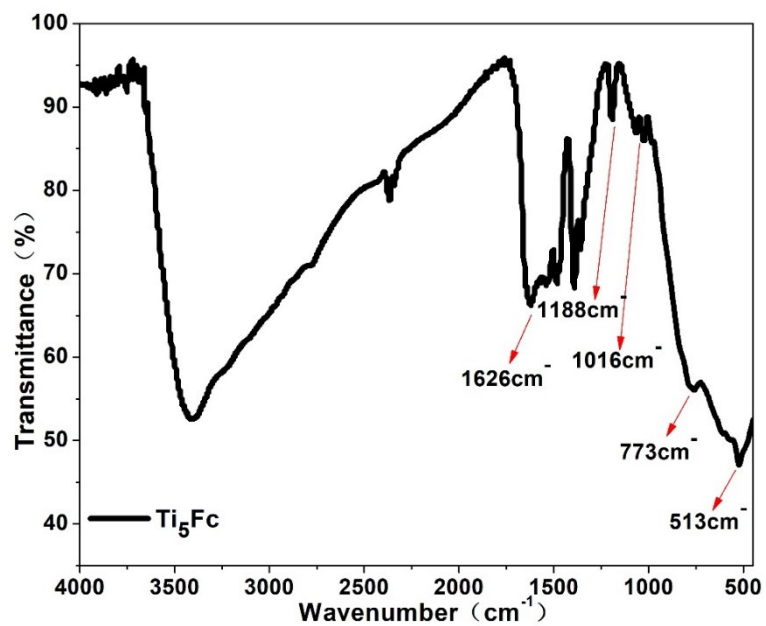


Figure S16. IR spectra of crystal sample of $\{\text{Ti}_5\text{Fc}\}$.

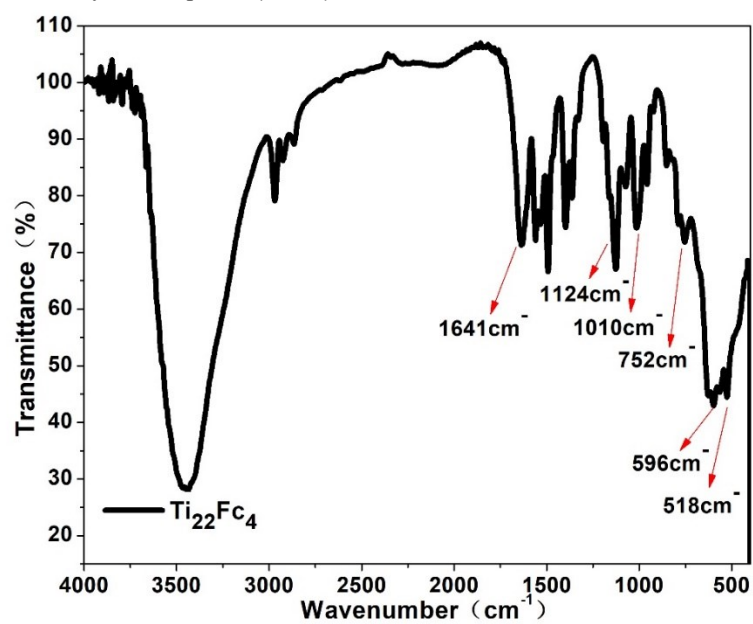


Figure S17. IR spectra of crystal sample of $\{\text{Ti}_{11}\text{Fc}_2\}$.

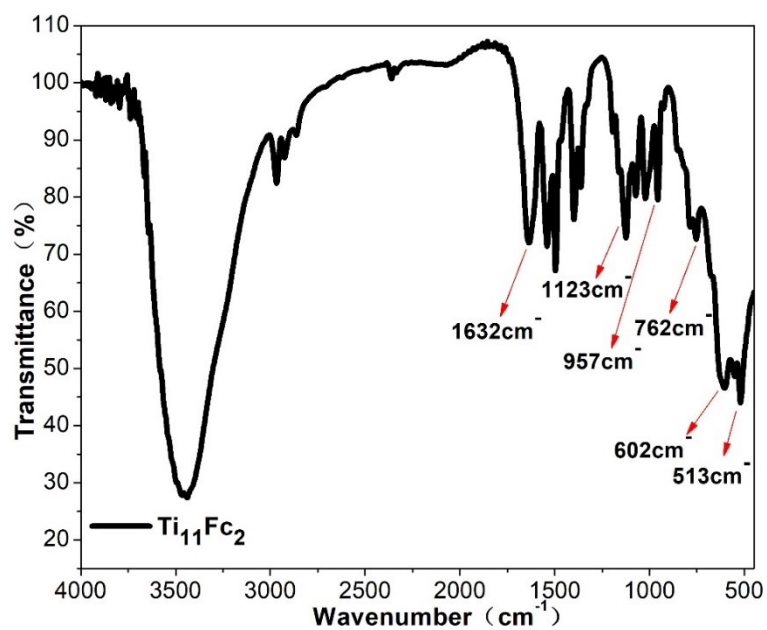


Figure S18. IR spectra of crystal sample of $\{\text{Ti}_{22}\text{Fc}_4\}$.

7. TG-Measurement

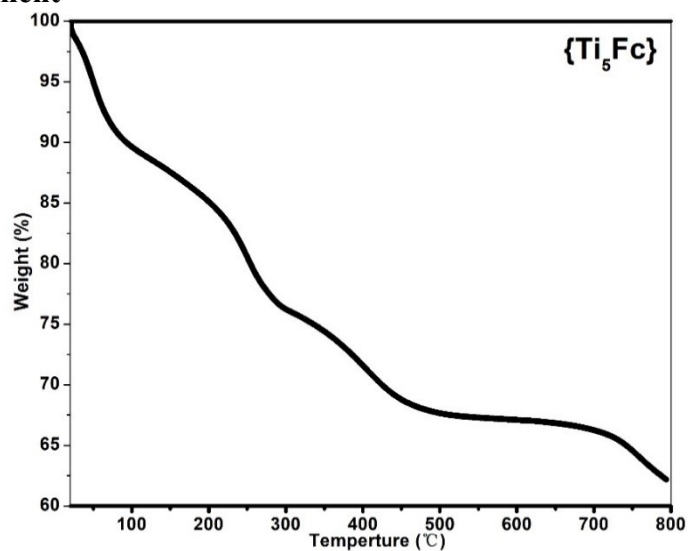


Figure S19. Thermal decomposition curve of $\{\text{Ti}_5\text{Fc}\}$.

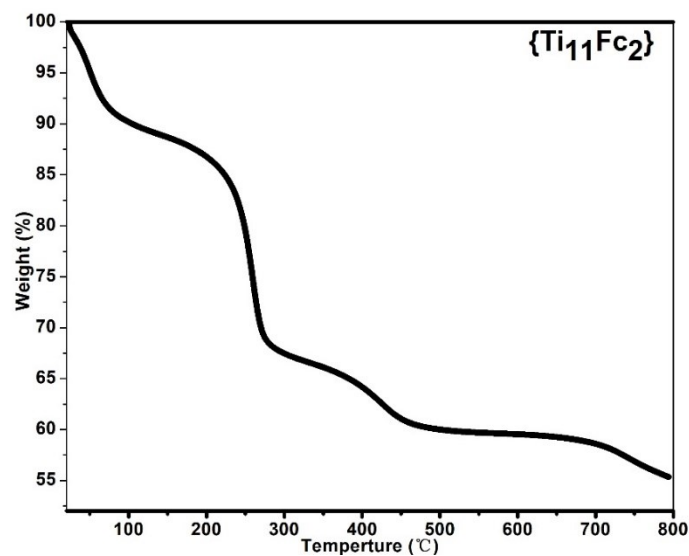


Figure S20. Thermal decomposition curve of $\{\text{Ti}_{11}\text{Fc}_2\}$

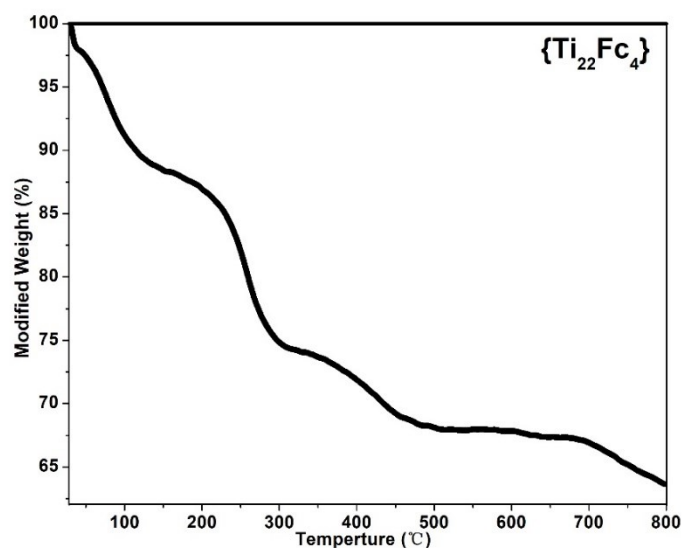


Figure S21. Thermal decomposition curve of $\{\text{Ti}_{22}\text{Fc}_4\}$.

8. ESI-MS measurements.

$\{\text{Ti}_5\text{Fc}\}$

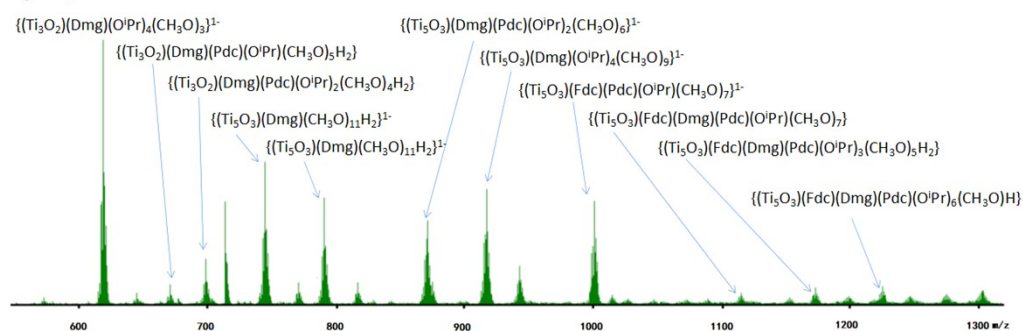


Figure S22. ESI-MS spectrum of the CH_3OH solution of $\{\text{Ti}_5\text{Fc}\}$.

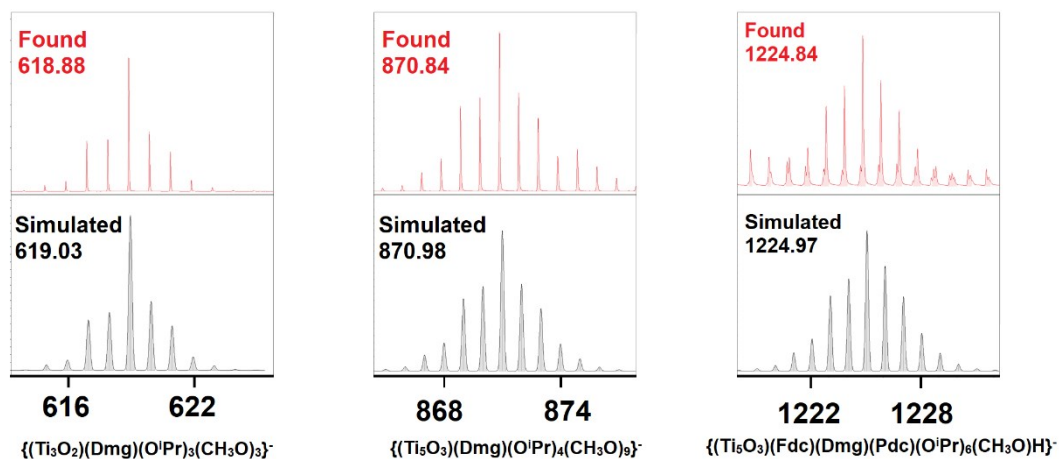


Figure S23. The isotope distributions of main peaks of ESI-MS spectrum of $\{\text{Ti5Fc}\}$.

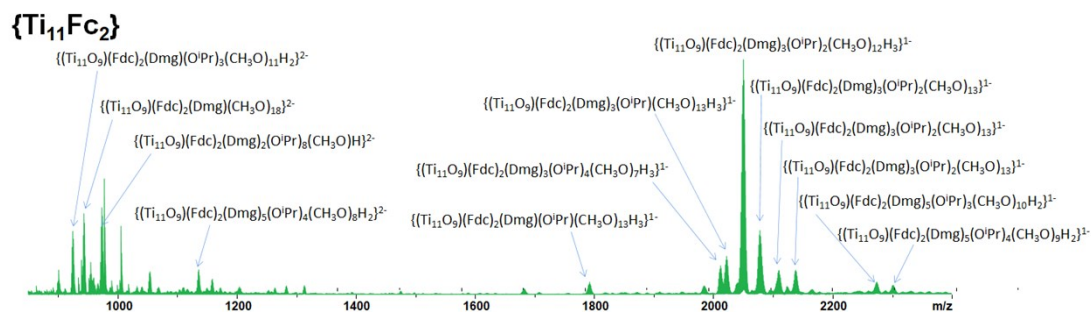


Figure S24. ESI-MS spectrum of the CH_3OH solution of $\{\text{Ti}_{11}\text{Fc}_2\}$.



Figure S25. The isotope distributions of main peaks of ESI-MS spectrum of $\{\text{Ti}_{11}\text{Fc}_2\}$.

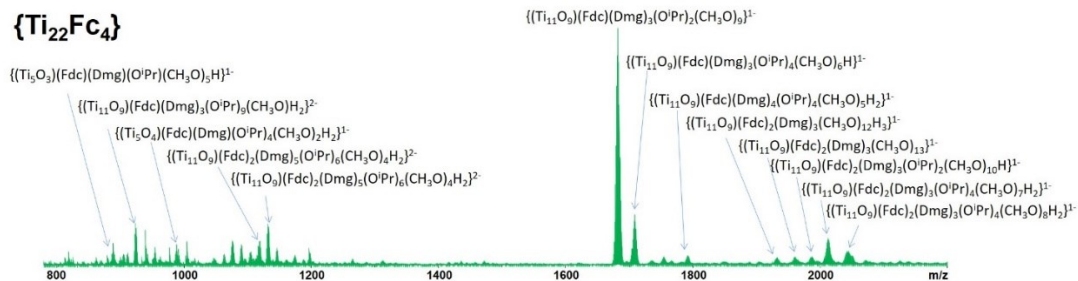


Figure S26. ESI-MS spectrum of the CH_3OH solution of $\{\text{Ti}_{22}\text{Fc}_4\}$.

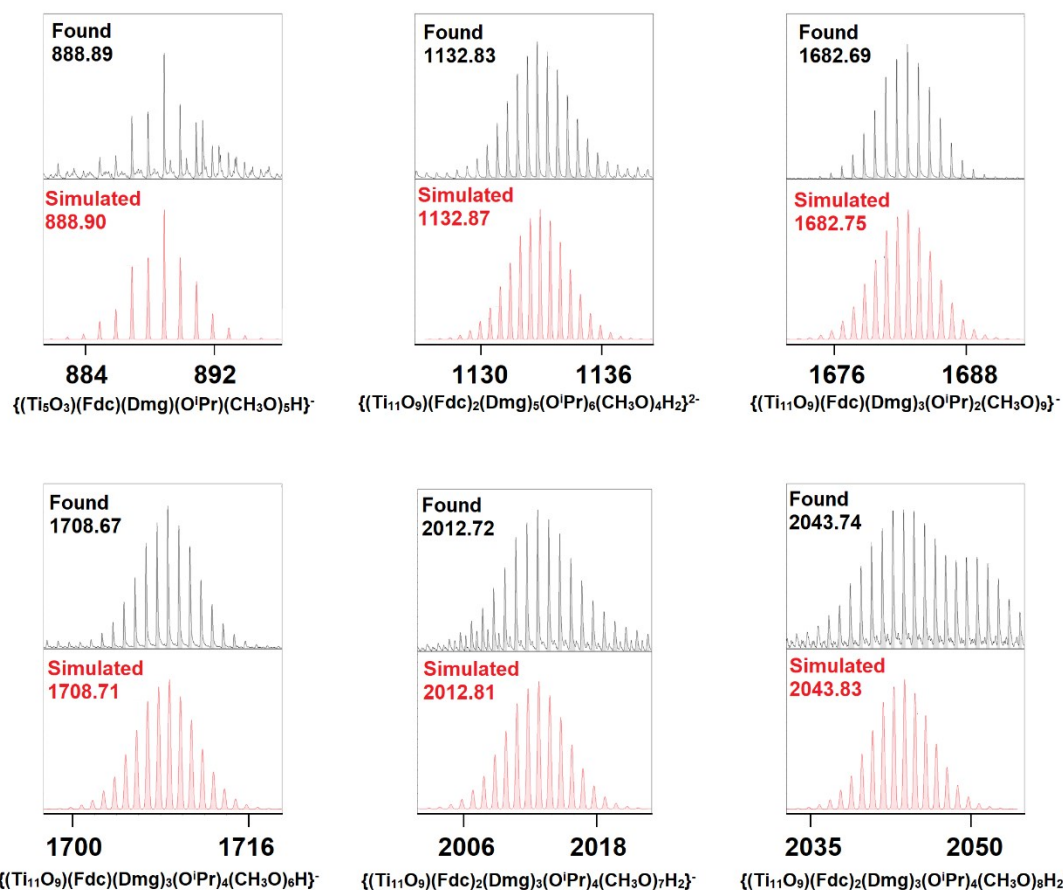


Figure S27. The isotope distributions of main peaks of ESI-MS spectrum of $\{\text{Ti}_2\text{Fc}_4\}$.

10 Photocatalysis

Table S2. The optimization of different reaction conditions of benzylamine to N-benzylidene-1-phenylmethanamine ^a

| Entry | Cat. | Sol. | Temp.(°C) | TBHP(μL) | Yield(%) ^b |
|-----------------|---------------------------------|------------------------|-----------|-----------------------------------|-----------------------|
| 1 | $\{\text{Ti}_5\text{Fc}\}$ | CH_3CN | 70 | 300 | 99 |
| 2 | none | CH_3CN | 70 | 300 | 12 |
| 3 | $\{\text{Ti}_5\text{Fc}\}$ | CH_3CN | 70 | 0 | 4 |
| 4 | $\{\text{Ti}_5\text{Fc}\}$ | CH_3CN | 70 | (H_2O_2) 300 | 2 |
| 5 | $\{\text{Ti}_5\text{Fc}\}$ | CH_3CN | 70 | (O_2) 1 atm | 3 |
| 6 | $\{\text{Ti}_5\text{Fc}\}$ | CH_3CN | 70 | 100 | 59 |
| 7 | $\{\text{Ti}_5\text{Fc}\}$ | CH_3CN | 70 | 200 | 79 |
| 8 ^c | $\{\text{Ti}_5\text{Fc}\}$ | CH_3CN | 70 | 350 | 92 |
| 9 | $\{\text{Ti}_5\text{Fc}\}$ | CH_3CN | 45 | 300 | 94 |
| 10 | $\{\text{Ti}_5\text{Fc}\}$ | CH_3CN | 20 | 300 | 88 |
| 11 | $\{\text{Ti}_5\text{Fc}\}$ | Ethanol | 70 | 300 | 80 |
| 12 | $\{\text{Ti}_5\text{Fc}\}$ | Toluene | 70 | 300 | 77 |
| 13 | $\{\text{Ti}_5\text{Fc}\}$ | 1,4-Dioxane | 70 | 300 | 12 |
| 14 | $\{\text{Ti}_5\text{Fc}\}$ | DMF | 70 | 300 | 65 |
| 15 | $\{\text{Ti}_5\text{Fc}\}$ | DMSO | 70 | 300 | 40 |
| 16 ^d | $\{\text{Ti}_5\text{Fc}\}$ | CH_3CN | 70 | 300 | 27 |
| 17 | $\{\text{Ti}_{11}\text{Fc}_2\}$ | CH_3CN | 70 | 300 | 95 |

| | | | | | |
|----|-------------------------------------|--------------------|----|-----|----|
| 18 | {Ti ₂₂ Fc ₄ } | CH ₃ CN | 70 | 300 | 90 |
|----|-------------------------------------|--------------------|----|-----|----|

^a Reaction conditions: substrate, benzylamine (110 μL, 1 mmol); catalyst (0.02 mmol); solvent (2 mL); TBHP=tert-butyl hydroperoxide; 12 h. ^b Determined by GC analysis and ¹H NMR, and the selectivity of imine is over 99% unless specifically mentioned. ^c Convention of benzylidene is 99%, selectivity of *N*-benzylidene-1-phenylmethanamine is 95%. ^d Using sunlight replaces Xe lamp.

Table S3. The time conversion for benzylamine to *N*-benzylidene-1-phenylmethanamine under the optimization condition ^a

| Entry | Cat. | Oxidant | Time | Addition | Yield ^b |
|-------|-------------------------------------|---------|------|----------|--------------------|
| 1 | {Ti ₅ Fc} | TBHP | 3 | None | 50% |
| 2 | {Ti ₅ Fc} | TBHP | 5 | None | 81% |
| 3 | {Ti ₅ Fc} | TBHP | 8 | None | 95% |
| 4 | {Ti ₅ Fc} | TBHP | 10 | None | 98% |
| 5 | {Ti ₅ Fc} | TBHP | 12 | None | 99% |
| 6 | {Ti ₁₁ Fc ₂ } | TBHP | 3 | None | 52% |
| 7 | {Ti ₁₁ Fc ₂ } | TBHP | 5 | None | 76% |
| 8 | {Ti ₁₁ Fc ₂ } | TBHP | 8 | None | 88% |
| 9 | {Ti ₁₁ Fc ₂ } | TBHP | 10 | None | 93% |
| 10 | {Ti ₁₁ Fc ₂ } | TBHP | 12 | None | 95% |
| 11 | {Ti ₂₂ Fc ₄ } | TBHP | 3 | None | 50% |
| 12 | {Ti ₂₂ Fc ₄ } | TBHP | 5 | None | 76% |
| 13 | {Ti ₂₂ Fc ₄ } | TBHP | 8 | None | 85% |
| 14 | {Ti ₂₂ Fc ₄ } | TBHP | 10 | None | 89% |
| 15 | {Ti ₂₂ Fc ₄ } | TBHP | 12 | None | 90% |

^a Reaction conditions: substrate, benzylamine (110 μL, 1 mmol), catalyst (0.02 mmol), TBHP (300 μL), solvent (2 mL), Xe lamp. ^b Determined by GC analysis and ¹H NMR.

Table S4. The optimization of different reaction conditions of benzylamine to *N*-benzylidene-1-phenylmethanamine ^a

| Entry | Cat. | Oxidant | Time | Addition | Yield ^b |
|-------|----------------------------------|---------|------|--------------------------------------|--------------------|
| 1 | {Ti ₅ Fc} | TBHP | 12 | benzoquinone | 42% |
| 2 | {Ti ₅ Fc} | TBHP | 12 | EDTA-2Na | 56% |
| 3 | {Ti ₅ Fc} | TBHP | 12 | Mn(CH ₃ COO) ₂ | 47% |
| 4 | Fc | TBHP | 70 | 300 | 12 |
| 5 | TiO ₂ | TBHP | 70 | 300 | 18 |
| 6 | Fc+TiO ₂ ^c | TBHP | 12 | None | 40% |

^a Reaction conditions: substrate, benzylamine (110 μL, 1 mmol), catalyst (0.02 mmol), TBHP (300 μL), solvent (2 mL), Xe lamp. ^b Determined by GC analysis and ¹H NMR. ^c The mixture were obtained by grinding of Fc and TiO₂ with the molar ratio of 1:1.

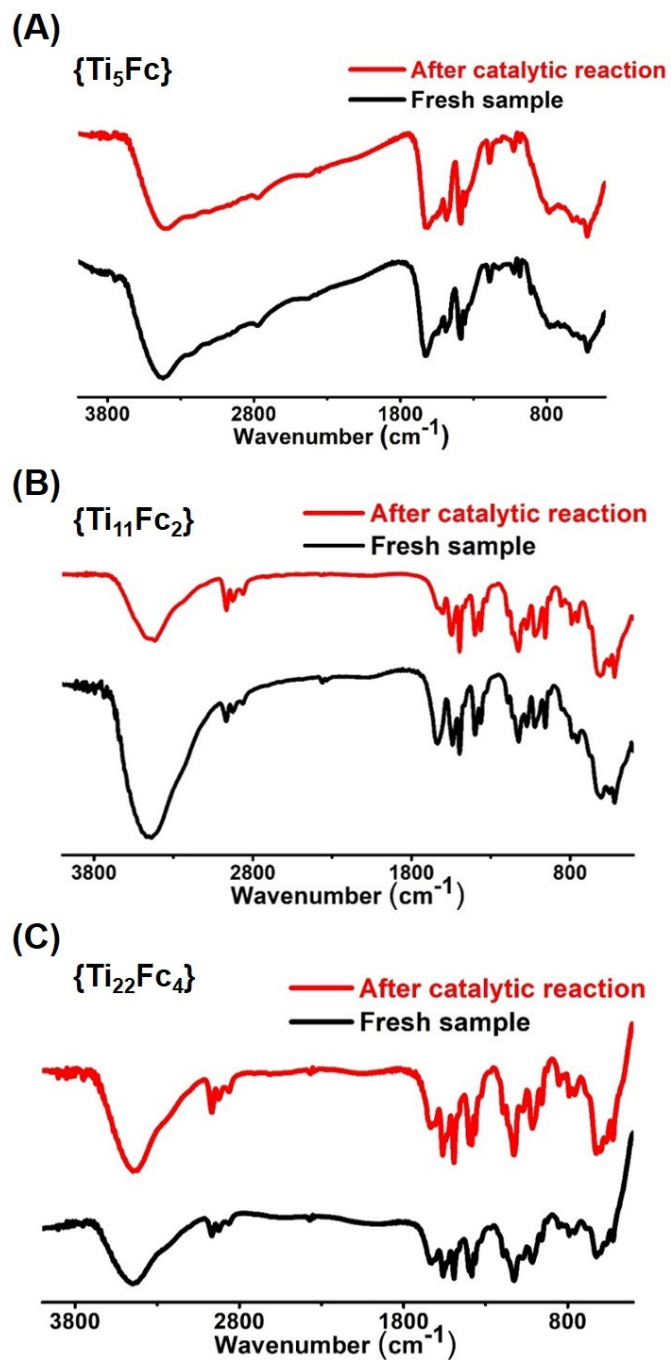


Figure S28. The IR spectrum of $\{\text{Ti}_x\text{Fc}_y\}$ before and after reaction.

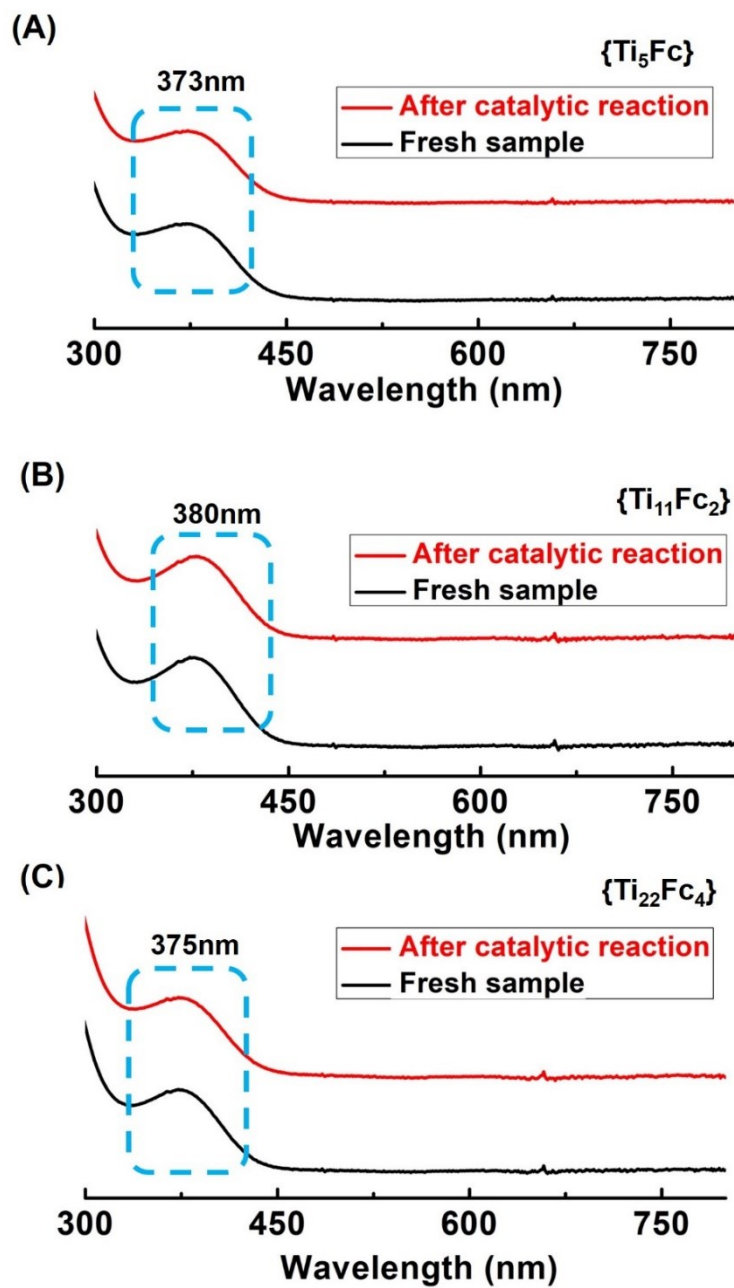


Figure S29. The solution-state UV-Vis spectra of three clusters before and after reaction.

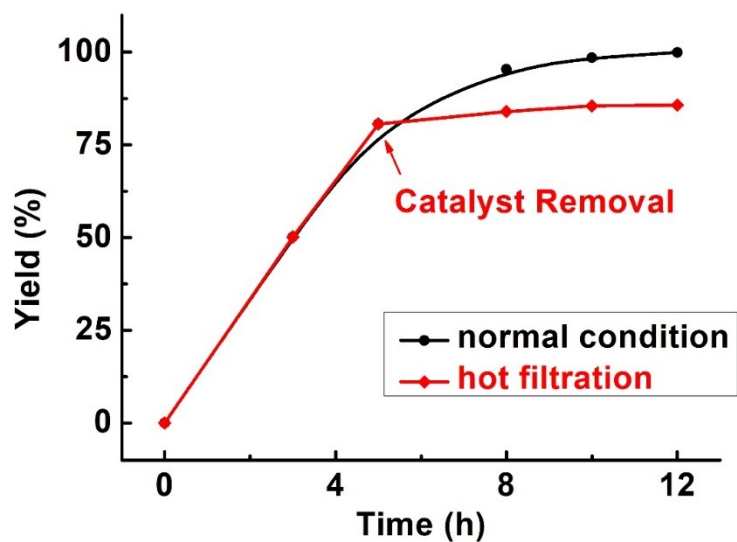


Figure S30. Hot-filtration test of benzylamine oxidation reaction catalytic by $\{\text{Ti}_5\text{Fc}\}$ at optimal condition.

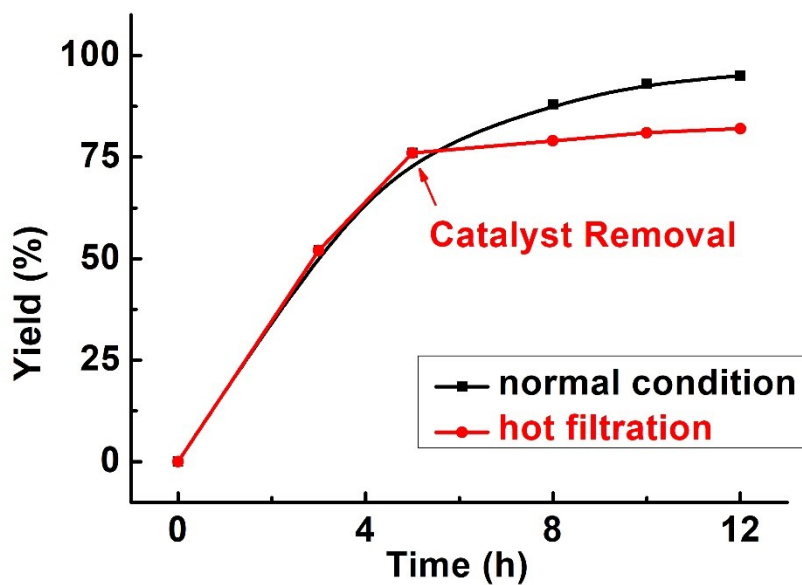


Figure S31. Hot-filtration test of benzylamine oxidation reaction catalytic by $\{\text{Ti}_{11}\text{Fc}_2\}$ at optimal condition.

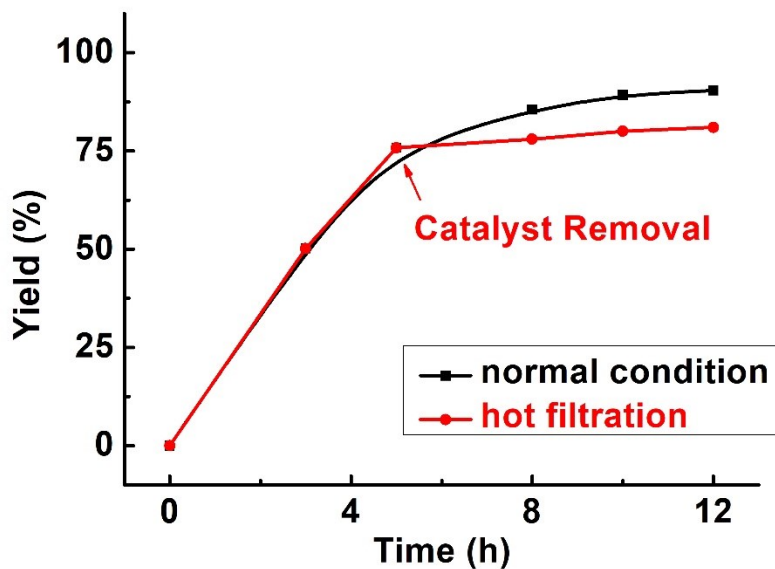


Figure S32. Hot-filtration test of benzylamine oxidation reaction catalytic by $\{\text{Ti}_{12}\text{Fc}_4\}$ at optimal condition.

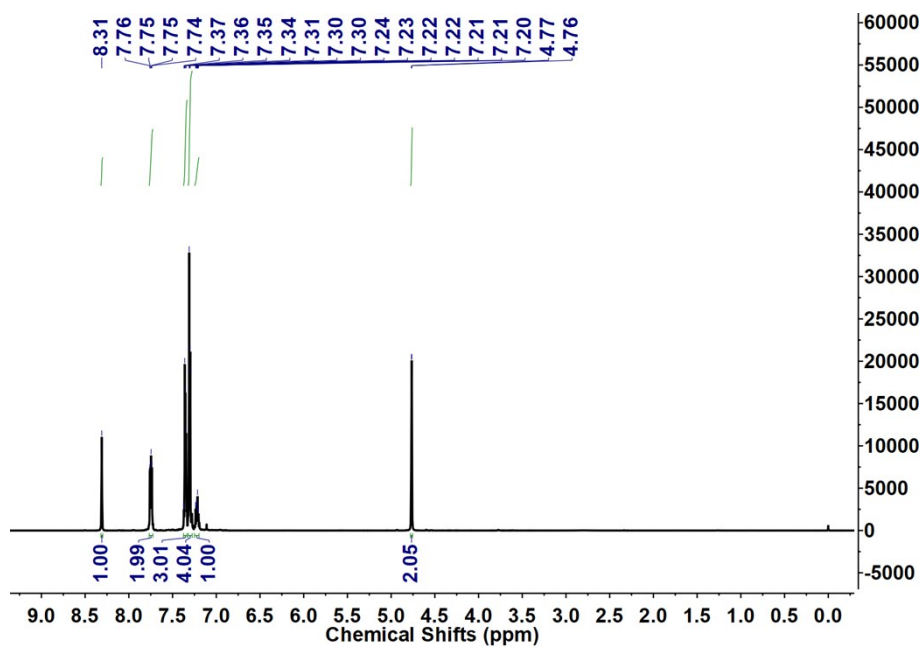


Figure S33. The ^1H NMR spectra of N-benzylidene-1-phenylmethanamine.

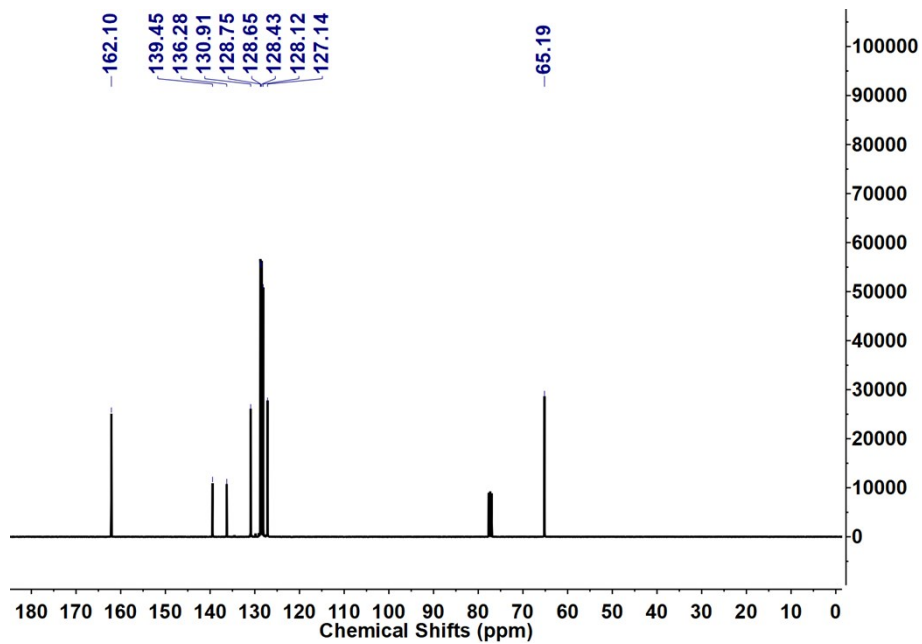


Figure S34. The ^{13}C NMR spectra of *N*-benzylidene-1-phenylmethanamine.